The EUMETSAT
Network of
Satellite Application
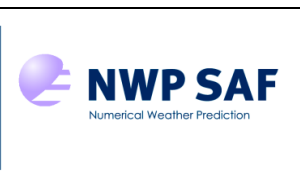Facilities

NWP SAF
Numerical Weather Prediction

Document NWPSAF_MO_VS_050

Version 1.0

13/10/14

The RTTOV UWiremis module Investigation into the angular dependence of IR surface emissivity

Eva Borbas

Met Office

ECMWF

Royal Netherlands
Meteorological Institute
*Ministry of Transport, Public Works
and Water Management*

METEO FRANCE
Toujours un temps d'avance

The RTTOV UWiremis module
Investigation into the angular dependence of IR surface emissivity

Eva Borbas

Space Science and Engineering Center, University of Wisconsin, USA

This documentation was developed within the context of the EUMETSAT Satellite Application Facility on Numerical Weather Prediction (NWP SAF), under the Cooperation Agreement dated 29 June 2011, between EUMETSAT and the Met Office, UK, by one or more partners within the NWP SAF. The partners in the NWP SAF are the Met Office, ECMWF, KNMI and Météo France.

Change record			
Version	Date	Author / changed by	Remarks
1.0	13/10/14	E. Borbas	

THE RTTOV UWIREMIS MODULE

INVESTIGATION INTO THE ANGULAR DEPENDENCE OF IR SURFACE EMISSIVITY

EVA BORBAS
SPACE SCIENCE AND ENGINEERING CENTER, UNIVERSITY OF WISCONSIN, MADISON, WI, USA

SCIENCE DOCUMENTATION

EUMETSAT, NWP SAF AS MISSION
NWP_AS13_P01

Change record			
Version	**Date**	**Author/changed by**	**Remarks**
0.1	Mar/3/2014	E. Borbas (UW/SSEC)	Initial draft
0.2	Oct/3/2014	E. Borbas(UW/SSEC)	
0.3	Oct/12/2014	R. Saunders (Met Office)	Minor comments
0.4	Oct/13/2014	E.Borbas(UW/SSEC)	Final version

Table of Contents

Scope

This document describes the scientific approach to a study that was performed by Principal Investigator Dr. Eva Borbas at the University of Wisconsin-Madison Space Science and Engineering Center (UW-SSEC) under contract to the EUMETSAT NWP-SAF between 1 April and 31 December 31 2013. This is a continuation of a previous NWP SAF AS mission during which an RTTOV IR emissivity (RTTOV-UWiremis) module and IR global land surface emissivity atlas have been developed for RTTOV 10. The UWiremis module provides a monthly mean and variance of the IR land surface emissivity at high spectra resolution. The objective of this new study was to investigate if the IR emissivity depends on the satellite zenith angle and, if there is a significant effect, to develop a parameterization correction to the RTTOV UW IREMIS atlas for input to RTTOV (v12 and later). The RTTOV fast radiative transfer model is a key NWP-SAF deliverable used in simulating the Earth emitted radiance at the top of the atmosphere as observed by operational weather satellites. Providing improved techniques for simulating infrared radiances over land using RTTOV is an important goal.

1. Introduction

Laboratory measurements (Label and Stoll, 1991) of bare soil show that a decrease in the IR emissivity with increasing viewing angle does exist. The magnitude of this effect, besides the optical properties of the materials, depends on the scattering mechanism, grain size, porosity, etc. ATSR experimental studies (Sobrino and Cuenca, 1999, Cuenca and Sobrino, 2004) also show the angular variation of thermal infrared emissivity in the 8- 14 μm spectral band for clay, sand, and gravel (~ 1-3% for 0 to 65 degrees), but homogeneous grass, for example, does not show angular dependence. Both studies agree that the 8-9 μm restrahlen bands are the most sensitive to the angular dependence, and the sand sample shows the greatest variation.

Garcia-Santos et al. (2012) also investigated the angular effect of emissivity on eight samples of inorganic soils between 7.7 and 14.3 μm. They found that the zenithal emissivity change was small for viewing angles less than 40 degrees, but after which the emissivity decreased significantly and that sand and quartz had the most influential factors. This work also established a relationship to take into account the zenithal dependencies for soil types. They also investigated the impact of ignoring the emissivity angular effects on retrievals of Land Surface Temperature using a split-window-type algorithm, and of outgoing long wave radiation. Systematic errors between 0.4K and 1.3K for LST and errors between 2 and 8 % in the surface energy balance were shown.

Ruston et al, (2008) investigated the viewing angle dependence on real HIRS observations. For viewing zenith angles less than 40 degrees, they found its effect was less than 0.3 % globally. They concluded that a simple correction could be made to the IR emissivity to account for the zenith angle dependence.

The RTTOV UWiremis Database is based on the monthly mean MODIS Emissivity products (MOD11), but that database does not include enough information to perform a viewing angle dependence study since the daily emissivity is a day-night mean. The database will include a day-night separated emissivity data when a new version known as Collection 6 of the MOD11 product will be released in 2014. For this reason, the UW dual regression AIRS/CRIS/IASI emissivity retrieval algorithm (Smith et al, 2011) that is a part of the Community Software Processing Package (CSPP, http://cimss.ssec.wisc.edu/cspp/) was used for this study instead. This algorithm is very suitable for this investigation since it retrieves the surface emissivity for all the channels providing very high spectral resolution spectra and the satellite zenith viewing angles can easily be extracted. The study was performed (see Section 2) using four months of data (representing the four seasons) over different surface types assuming the emissivity does not change over the sample time period (month). In section 3 the retrieved CrIS IR emissivity spectra were investigated as a function of satellite zenith angle separated by day and night and compared to the RTTOV IR emissivity atlas (which is the modified UW HSR emissivity database) to estimate the magnitude of the angular dependence. As a result, a satellite zenith angle correction function depending on the surface type and wavelength was developed (Section 4). The correction function was evaluated on in-situ aircraft measurements (Section 5) and four selected global day of IASI observations (Section 6). Two sets of simulated brightness temperatures were compared to the observed data by using the current RTTOV IR emissivity atlas with and without applying the satellite zenith angular corrections. The report ends with the summary and conclusions in Section 7.

2. Collecting data for angular study

To investigate the satellite zenith angular dependence of the IR land surface emissivity data, data from the Cross-track Infrared Sounder (CrIS), a Fourier transform spectrometer, has been selected. CrIS has 1305 spectral channels over 3 wavelength ranges: LWIR (9.14 - 15.38 μm); MWIR (5.71 - 8.26 μm); and SWIR (3.92 - 4.64 μm). CrIS scans a 2200 km swath width (+/- 50 degrees of scanning angle), with 14 km nadir spatial resolution.

Four months of CrIS data have been processed by the modified version of the UW dual regression AIRS/CRIS/IASI retrieval algorithm Version 1.2 (Smith et al, 2011) which is a part of the Community Software Processing Package (CSPP, http://cimss.ssec.wisc.edu/cspp/). The four months (April, July and October 2012 and January 2013) have been selected to be able to capture any seasonal changes. The CSPP Dual Regression (DR) Algorithm was run over clear sky conditions only on a single field of view. The retrievals were separated by land/ocean and day/night. Polar regions over 70 degrees latitude were eliminated from the study.

From previous literature we know that the angular dependence on the laboratory measurements highly depends on the surface types. To get the surface type categorization, the 1 km spatial resolution International Geosphere-Biosphere Program (IGBP) Ecosystem Database (*http://edc2.usgs.gov/glcc/globdoc2_0.php* , *Belward, 1996*) has been remapped to 5 km resolution and used. The IGBP16, Barren/Desert Land category has been split due to the location and different material of the surface (distinguish from the sandy soil type). The

IGBP16 above 60 degrees latitude has been defined as IGBP17 (which is originally "Ocean water" category, and it is not used for this land application).
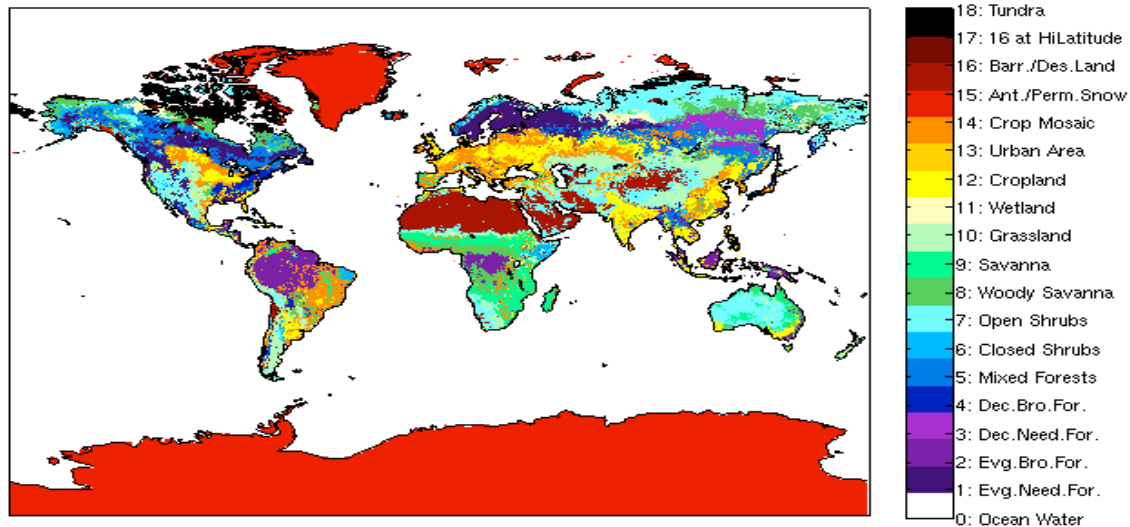

Figure 1: The IGBP Ecosystem map (right) with the name of the categories (left).

3. Investigating the IR land surface emissivity angular dependence

First of all, to see if the IR land surface emissivity has any angular dependence, we focused on a certain homogenous surface type (sand desert area) and time (see Section 3a) and then in Section 3b we extended our study to all 18 IGBP ecosystem categories and all seasons (four selected months).

a. Angular dependence of the surface IR emissivity and the skin temperature

To investigate the angular dependence of the CrIS DR clear sky emissivity retrievals, first a homogenous, non-vegetated area was selected over the Sahara desert. The IGBP eco-system category 16, Barren/Desert Land over the globe with red points is shown in Figure 2 and our selected investigated area is boxed in yellow.
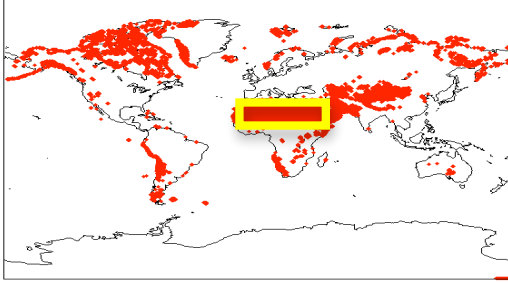
Figure 2: Location of the IGBP category 16: Barren/Desert land. The investigated area is indicated by the yellow box.

First, all the collected clear sky CrIS Emissivity retrievals in January 2013 were plotted on Figure 3a against the satellite zenith angles for four selected wavelengths: 3.7, 4.3. 8.3 and 12.1 μm - representing the short, middle and long IR wavelength regions - separated by daytime (red) and nighttime (blue). The emissivity values were grouped into one-degree bins. The means of these emissivity bins are plotted with a thin black line on each panel along with the fitted second-degree polynomial curve (thick black line). The IR emissivity at the short and middle wavelengths shows the most variation generally, but also as the satellite zenith angle changes. The difference between the mean emissivity at nadir (0 degrees) and the maximum of 60 degrees shows a 6.8 % and 8.0 % increase for the 3.7 and 4.3 μm respectively over daytime and 3.2 % and 6.4 % over nighttime. A larger variation in the short wavelength is expected, because of the solar contamination of this IR region. For the same reason these variations should be smaller over night. The IR emissivity over sand desert is very sensitive and varies significantly around the 8.3 μm – the so-called restrahlen band. In our study this band shows a 5.4 % increase over daytime and does not show significant angular change over night. Over the long wave region, the land surface emissivity does not vary much, so the angular changes are much smaller as well. Decreases of 1.1 % and 0.9 % in emissivity were observed at 12. 1 μm.

When a similar figure to Figure 3a is created but for the RTTOV UWiremis database (Figure 3b), as expected, no angular dependence can be seen at any wavelength. The monthly mean emissivity database averages out all the variation from the satellite zenith angles.

The polynomial fitting (thick black curve) of the CrIS Emissivity retrievals was used to simulate the angular change of the RTTOV UWiremis database. The bias between the CrIS Emissivity and the RTTOV UWiremis database was also taken into account. Application of the angular correction function, which is described in more detail in Section 4, is demonstrated on Figure 3c. This figure is similar to Figure 3a and 3b, but the angularly corrected RTTOV UWirems is plotted over the same area, for the same month and the four selected wavelengths separated by day and night. The image shows that the angularly corrected RTTOV UWiremis database agrees well with the CrIS Emissivity retrievals.

To be sure that the IR emissivity angular dependence is real, the skin temperature should be independent from this effect. Figure 4 shows all the skin temperatures as a function of satellite zenith angle for the same selected time and area. The nighttime (right) panels show no variation at all from the satellite zenith angles. While the daytime image (left) shows a 2.3 % decrease between the nadir and 60 degree satellite zenith angle, we believe it is not significant and mostly due to much fewer sample numbers at high angles and the cooling shadow effect of the surface at high viewing angles. This may agree with the night time cases (right panel), where no variation is shown.
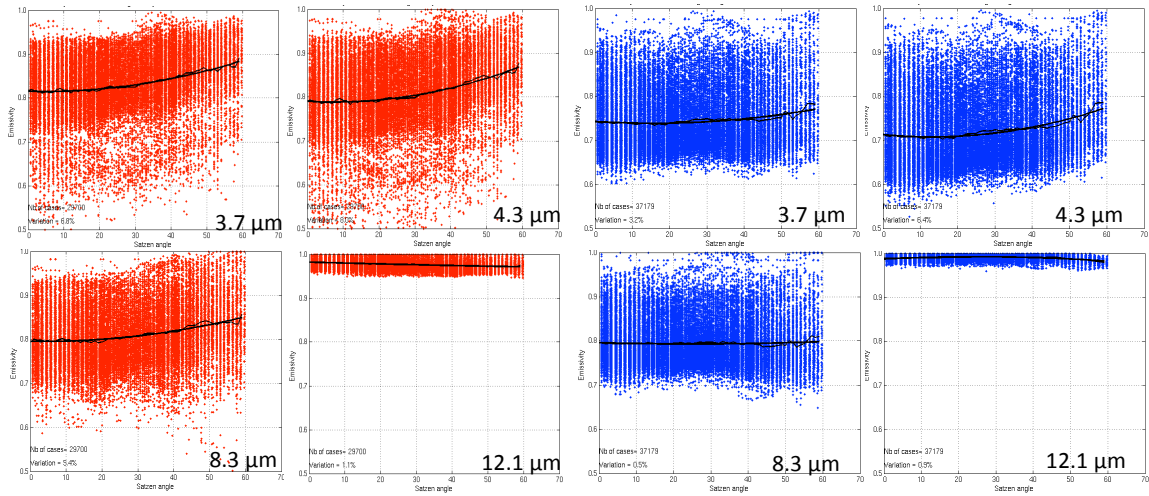
Figure 3a: Satellite zenith angular dependence of the CrIS Emissivity retrievals over the Sahara desert at four selected wavelengths in January 2013, separated by daytime (red) and nighttime (blue). The thin black line stands for the mean emissivity falling in the one-degree satellite zenith angle bins and the thick black line is its polynomial fitting curve.
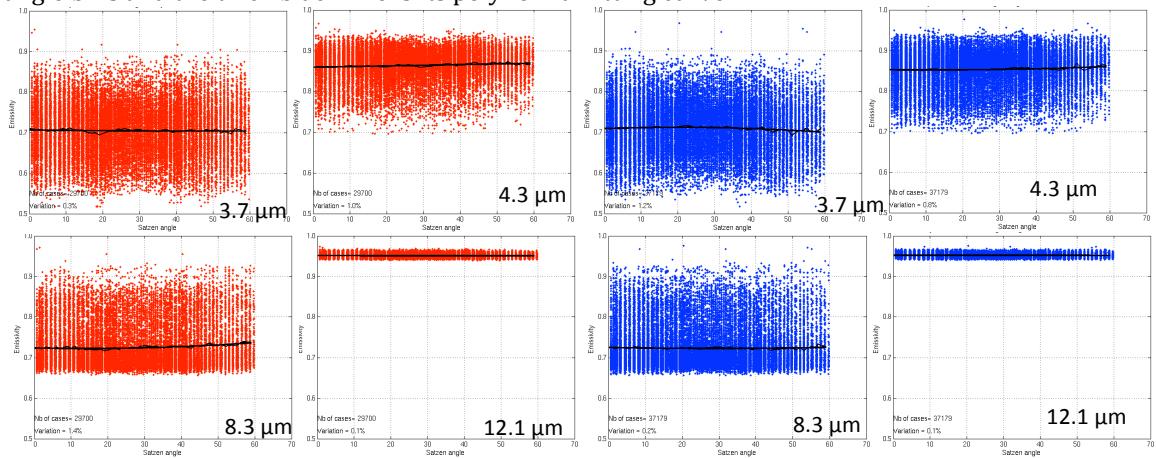
Figure 3b: Same as Figure 3a, but shows the angular independence of the UW Global IR Land Surface emissivity database.
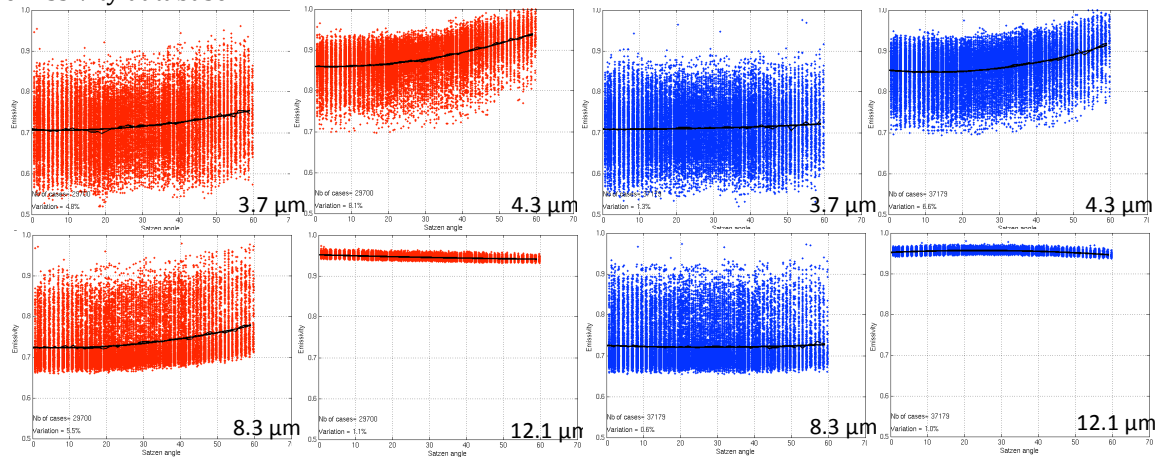
Figure 3c: Same as Figure 3b, but after applying the angular correction function on the UW Global IR Land Surface emissivity database.
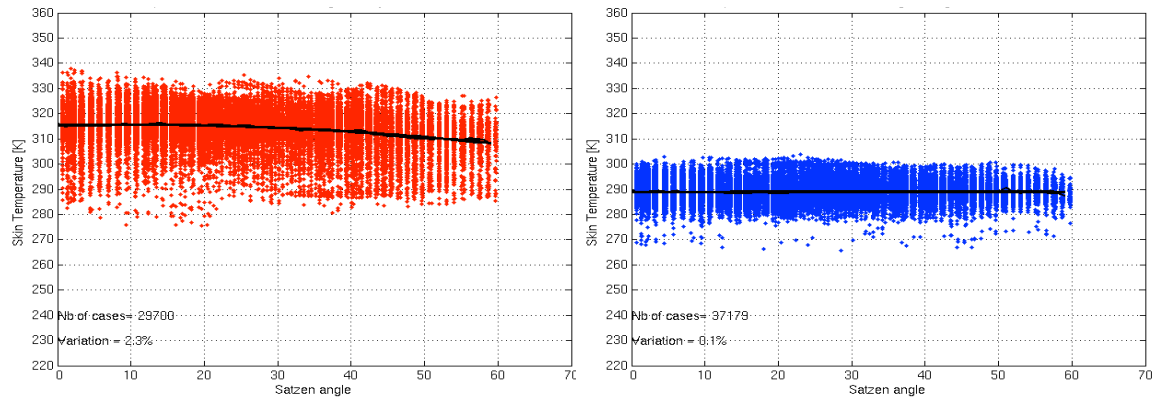
Figure 4: Angular dependence of the Skin Temperature for January 2013 over the Sahara desert.

b. Angular dependence by wavelengths and IGBP eco-systems

Before applying the angular correction function globally and for the four selected months, the angular changes were investigated for all 10 baseline fit hinge points: 3.6, 4.3, 5.0, 5.8, 7.6, 8.3, 9.3, 10.8, 12.1, and 14.3 μm. Note, that the hinge points were selected to capture IR emissivity spectral shapes in the best possible way.

The polynomial fitting curve of CrIS emissivity retrievals at the 10 hinge points are plotted in Figure 5 for the Barren/Desert Land (IGBP16) and the Savanna (IGBP09) ecosystem categories on January 2013 separated by day (left panels) and night time (right panels).
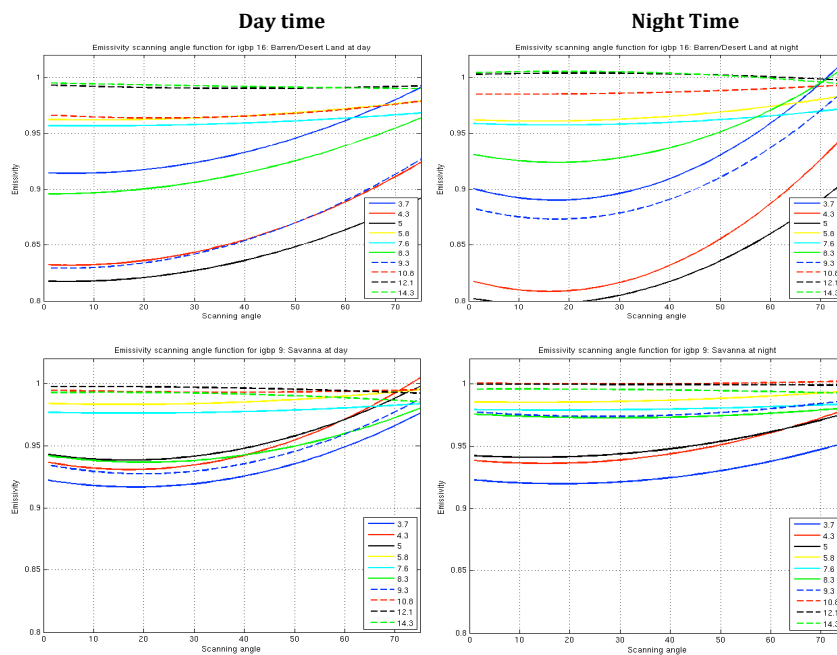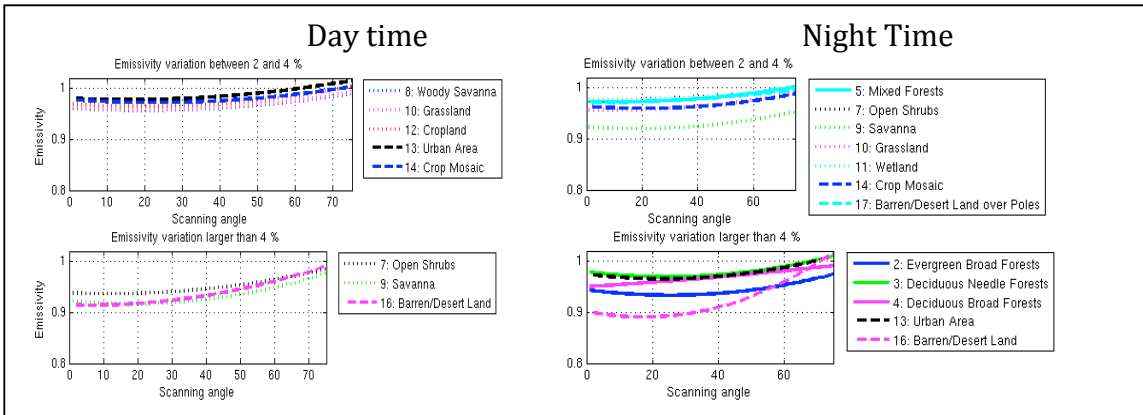

Figure 5: Emissivity changes by satellite zenith angle for IGBP16 (Barren/Desert Land, top two panels) and IGBP09 (Savanna, bottom two panels) at the 10 hinge points on January 2013.

8

The most sensitive hinge points were the following: 3.7, 4.3, 5, 8.3 and 9.3 μm. When the satellite zenith angle increased, the emissivity increased. However at 10.8 μm, the magnitude and direction of the slope of the emissivity depends on the IGBP ecosystem type. The longer wavelengths (12.1 and 14.3 μm) also show some changes, but with less magnitude and the emissivity mostly decreases with the satellite zenith angle. To investigate the direction and magnitude of changes, these polynomial fitting curves are further studied for all the ecosystem categories and for all four seasons.

Emissivity changes (polynomial fitting curve of the CrIS Emissivity retrievals) on January 2013 by satellite zenith angle for each IGBP type over the globe are plotted at 3.7, 8.3 and 12.1 μm in Figure 6a, b, and c., respectively. The IGBP ecosystem types have been classified based on the emissivity change between the nadir and 60 degree satellite zenith angles. The fitting curve for a particular ecosystem is plotted if the emissivity difference between that at nadir and that at 60 degrees was between 2 and 4% (top panel) or was larger then 4% (bottom panel). In January 2013, at wavelength 12.1 μm, all the ecosystem types showed less than 2% changes by the satellite zenith angles; so instead, the July 2012 results are shown on Figure 6c. The most sensitive IGBP ecosystem categories are the Barren/Desert Land (16, less than 60^0 Latitude), Savanna (9), Open Shrubs (7), and at 12.1μm the Urban Area (13) type. In daytime, the less vegetated surface types are mostly dominated, while at nighttime, some forest types also show significant changes.

To see if any conclusions can be made regarding the direction of the emissivity changes as a function of wavelength (Y-axis) and ecosystem type (X-axis), the sign (-1 or +1) of the slope of the fitting curves was plotted for the 10 hinge points and all the IGBP ecosystems types for all four months separated by day- and nighttime (see Figure 7a and 7b). On these figures, only the significant changes are shown. The thresholds for determining significance have been set as 0.5 % for wavelengths less than 10.8 μm and 0.05 % for the longer wavelengths. Generally, we can conclude that for both day- and nighttime increasing changes occur at wavelengths less than 10.8 μm and decreasing changes at the longer wavelengths with the exception of the Urban Area (IGBP 13) for daytime spring and summer and the deciduous forests (IGBP 3 and 4) for night time winter and spring. In addition, the longer wavelengths decreasing change is more pronounced at night time than at daytime.

The differences in the IR emissivity angular changes shown above suggest the need to create an angular correction function as a function of surface type and wavelength, separated by season and day/night time. The following section (4) describes the proposed RTTOV UWiremis angular correction function in more detail.
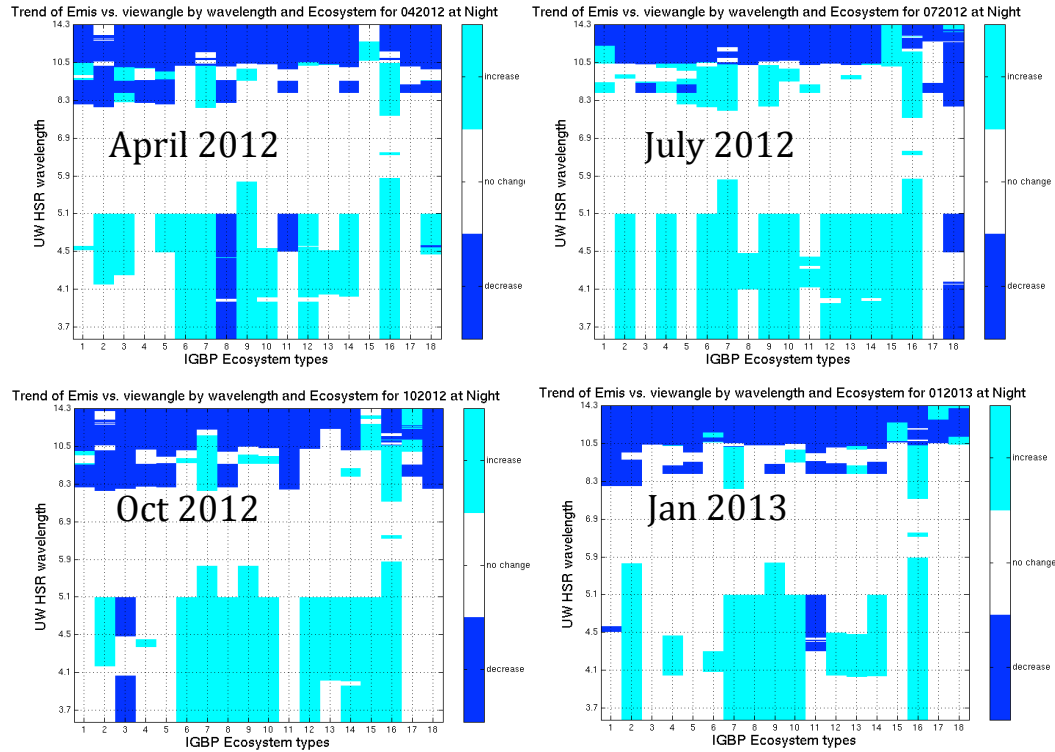
Figure 6a: IR Emissivity changes by satellite zenith angle for all the IGBP categories at 3.7 μm on January 2013. The angular fitting function is plotted for an IGBP ecosystem type if the emissivity difference between nadir and 60 degree was between 2 and 4 % (top panel) or was larger then 4 % (bottom panel). A missing panel means that there was no IGBP ecosystem type fulfilling that criterion.
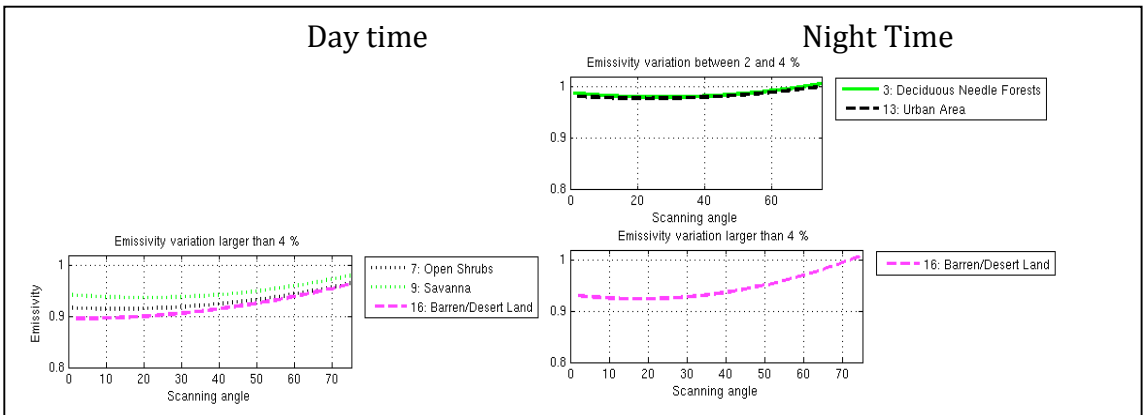

Figure 6b: same as Figure 6a, but at 8.3 μm. A missing panel means that there was no IGBP ecosystem type fulfilling that criterion.
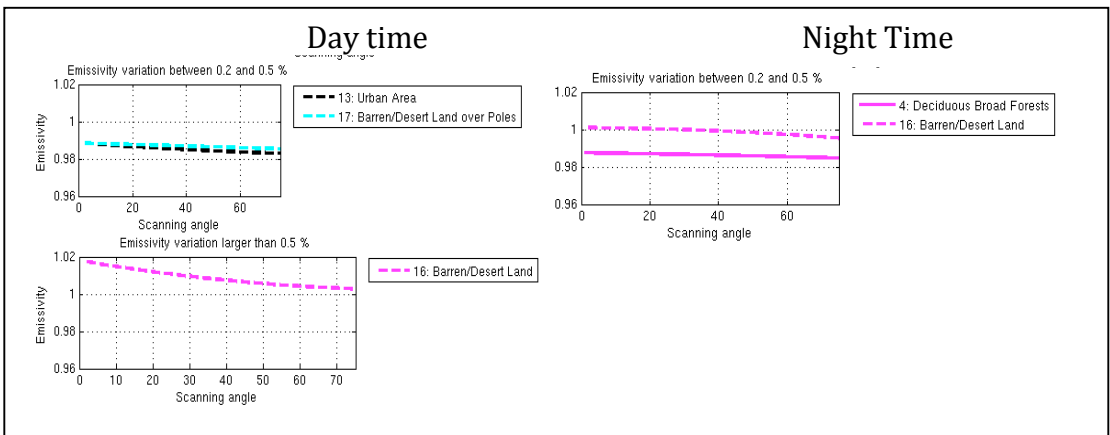
Figure 6c: same as Figure 6a, but at 12.1 μm and for July 2012. A missing panel means that there was no IGBP ecosystem type fulfilling that criterion.

Figure 7a: The sign of the emissivity change at nighttime by satellite zenith angle as a function of wavelengths (Y-axis) and IGBP ecosystem types (X-axis) for four months. Light blue stands for increasing and dark blue is for decreasing change. Only significant changes are shown. The thresholds for determining significance have been set as 0.5 % for wavelengths less than 10.8 μm and 0.05 % for the longer wavelengths.
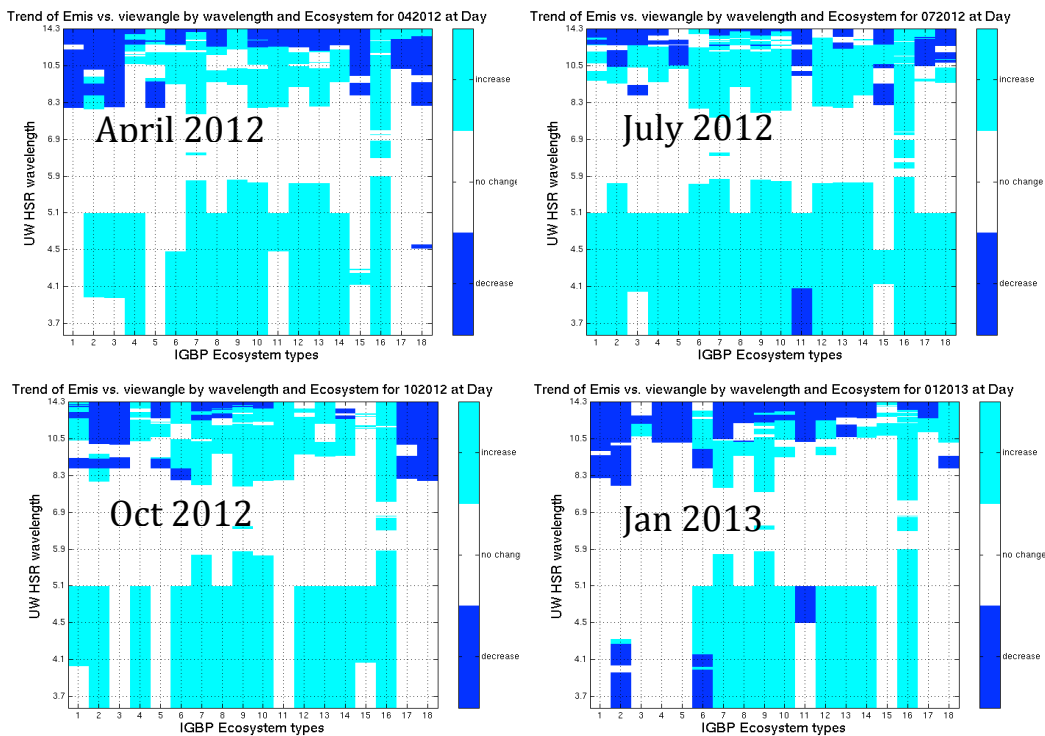
Figure 7b: same as Figure 7a, but for daytime.

4. Development of the RTTOV UWiremis angular correction function

Although the previous results were demonstrated on the ten hinge points, the CrIS emissivity retrievals on high spectral resolution were derived and used to create the second order polynomial fitting functions (F) for a certain satellite zenith angle (φ) as a function of wavelength (λ) and IGBP ecosystem type ($igbp$):

$$F(\lambda, igbp) = p_1 * \varphi^2 + p_2 * \varphi + p_3. \qquad \text{Eq. 1}$$

This fitting function has been calculated separately for day- (d) and nighttime (n) and for all four months, representing the four seasons. The dimensions of the $\mathbf{p_d}$ and $\mathbf{p_n}$ coefficients matrixes are the number of wavenumbers (416) and the number of IGBP ecosystem types (18).

The polynomial fitting function was used to get the angular correction function in the following way:

1. The satellite zenith angle (φ) is applied in Eq. 1 to get the $\mathbf{F}$ values for the IGBP surface type of the current pixel on high spectral resolution, using $\mathbf{p_d}$ or $\mathbf{p_n}$ coefficients according to the situation.
2. The differences ($\mathbf{dF(\lambda)}$) of the $\mathbf{F}$ values between those at nadir and at the actual φ satellite zenith angle are calculated for each spectral point.
3. The angular corrected emissivity is calculated as follows:

$$\mathcal{E}_{angcorr}(\lambda) = \mathcal{E}_{orig}(\lambda) * (1 - dF(\lambda)) \qquad \text{Eq. 2}$$

In order to use the angular correction function in RTTOV 11 and beyond, the coefficient matrixes ($\mathbf{p_d}$ and $\mathbf{p_n}$) have been stored in four separate netcdf files by season (*uwiremis_angcorr_2013xx.nc,* where xx= 01, 04, 07 and 10, 485 kB) . In addition, two new subroutines, the *rttov_uwiremis_read_angfunc* and the *rttov_uwiremis_angcorr* have been added.

5. Evaluation with campaign measurements

Our theory that the angular dependence differs with wavelength agrees with the Aircraft ARIES results. The mean of ARIES Emissivity retrievals with a nadir view and a viewing angle of 40º is shown on Figure 10. The aircraft measurements were taken over eastern England on 22 Sept 2010 (*Personal communication with Stuart Newman, Met Office, UK*). By increasing the view angle, the emissivity was decreased between the 760 (13.1 μm) and 1060 cm^{-1} (10.6 μm) and was increased between the 1060 and 1240 cm^{-1} (8.1 μm).
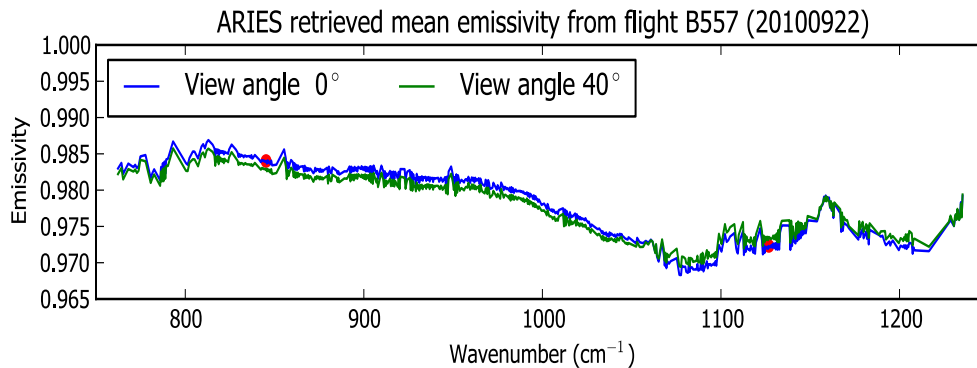
Figure 8: Mean aircarft ARIES emissivity retrieval where the measurements were taken at 0 (blue) and 40 degree (green) viewing angles over eastern England on 22 Sept 2010.

6. Evaluation with IASI calculated brightness temperatures

To evaluate the angular correction function of the RTTOV UWiremis module, IASI data have been chosen, where IASI represents a high spectral resolution IR instrument on a polar orbiting satellite (METOP-A). Brightness temperatures were calculated for 616 selected channels (NOAA/NESDIS selected subset) using the RTTOV UWiremis emissivity with and without the angular correction function for four selected global days in 2008 representing each season: Jan 15, Apr 14, July 15 and Sept 29. These two sets of simulated BTs then were compared to the collocated observed BTs over land pixels and clear sky conditions only. The following simplifications were applied during the calculations: snow fraction was not applied, and no other trace gases were added besides water vapor and ozone. To determine the clear conditions, the IASI 10.5, 11.5 and 12.5 μm BTs were used. The comparisons were further subdivided by day and night using the threshold of 85 degrees for the observed solar azimuth angle. The ECMWF 6 hour reanalyses fields at 0.5-degree spatial resolution were chosen for the forward calculations. To make the time collocation, one-hour time gaps were allowed for both night and day. For spatial collocations, the ECMWF grid points were bilinearly interpolated to the center of the IASI FOVs.

A case study on July 15, 2008, at 11:17 UTC (daytime) when the IASI granule passes over the Saudi Arabian desert region with high satellite zenith angles is shown on Figure 9. The IGBP ecosystem map shows that the land area is mostly in the Barren/Desert (igbp=16, red) or Open Shrubs (igbp=7, blue) category. The same granule case with biases over the whole IR spectrum is shown in the top panel of Figure 10; the biases are between the calculated and observed brightness temperatures when the RTTOV UWirmeis module without (black) and with the angular correction function (red) was used in the forward model calculation. Only pixels with a larger than 30 degree satellite zenith angle were counted, which means that in this case, all the land pixels were counted.
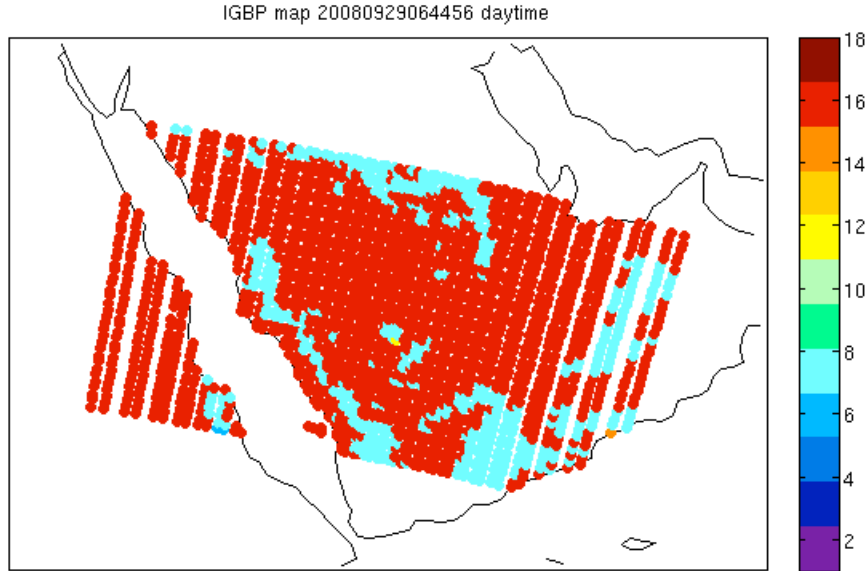
Figure 9: The IGBP ecosystem map on Sept 29, 2008 at 06:44 UTC (daytime).
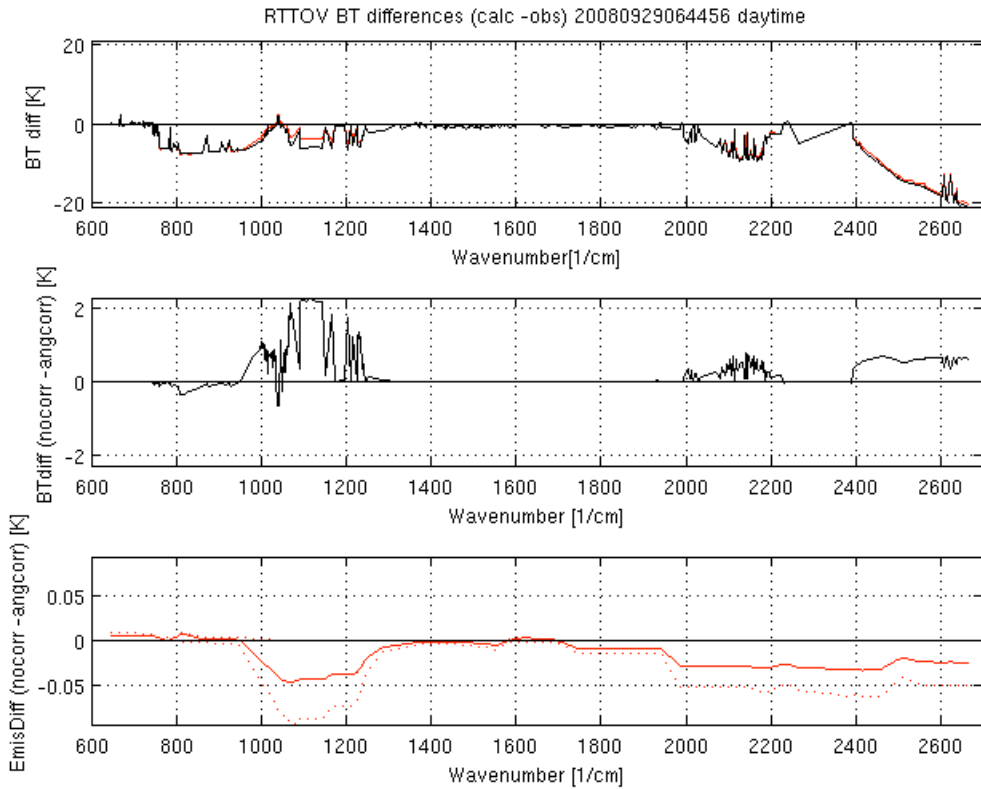

Figure 10: (top) The biases of the IASI BTs (calc-obs) (satzen angle > 30 degree) for granule overpass on Sept 29, 2008 at 06:44 UTC when RTTOV UWirmeis module without (black) and with the angular correction function (red) was used in the forward model calculation. (middle) The differences of the two curves in the top panels are shown. The positive values represent positive impact when the new angular correction function is used. (bottom) Mean emissivity differences between the original and angular corrected ones. Negative values mean emissivity increases with a satellite zenith angle increase. Standard deviation is also added to this panel.

The differences of these two biases are plotted in the middle panel of Figure 10. The positive values represent positive impact (reduced biases) when the new angular correction function is used. The bias has been reduced by 2.5 K between the 1050 cm^{-1} (9.5 μm) and 1250 cm^{-1} (9.5 μm) and by 1K between the 750 cm^{-1} (8μm) and 1050 cm^{-1} (9.5μm) spectral region. Mean emissivity differences between the original and angular corrected versions are also shown in the bottom panel of Figure 10. Positive values mean that the emissivity increases as the satellite zenith angle increases. The standard deviation is also included in this panel.

This case study represented only those situations where the greatest angular effect was expected: over the IGBP16 (Barren/Desert) or IGBP07(Open shrubs) categories with large satellite zenith angles. Overall statistics as a function of satellite zenith angle and IGBP surface type for all four days are presenting below.

In Figure 11a and b, the biases between the calculated and observed brightness temperatures of the *globally covered* Barren/Desert ecosystem type as a function of satellite zenith angle at the BF hinge points over night time are plotted for the four selected days.
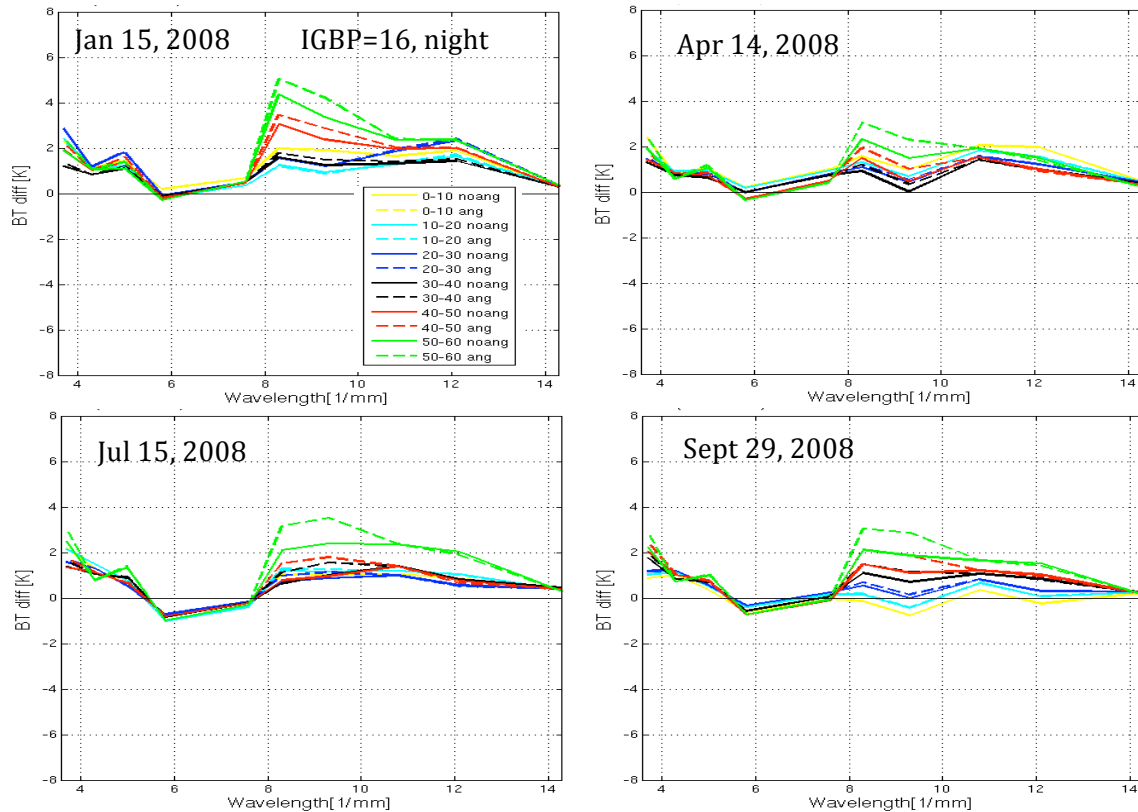
Figure 11a: Mean differences of the calculated and observed mean brightness temperatures as a function of satellite zenith angle for the Barren/Desert Land (IGBP=16) at the BF hinge points at **night time**. Solid lines represent the case when the viewing angle correction was not applied and dashed line shows the mean differences when the correction function has been applied in the forward model calculations.

The means between the calculated and observed BT differences were binned into 10 degree satellite zenith angle classes. Each color line represents an angle bin. Solid lines represent cases when the calculated brightness temperatures were obtained without applying the viewing angle correction and dashed lines when it was applied. The largest biases were obtained over the 8-10 micron Restrahlen band with the largest variation by satellite viewing angles. In this spectral region, the biases (calculated – observed BTs) are almost all positive, which means at night time the angle correction application degrades the results.
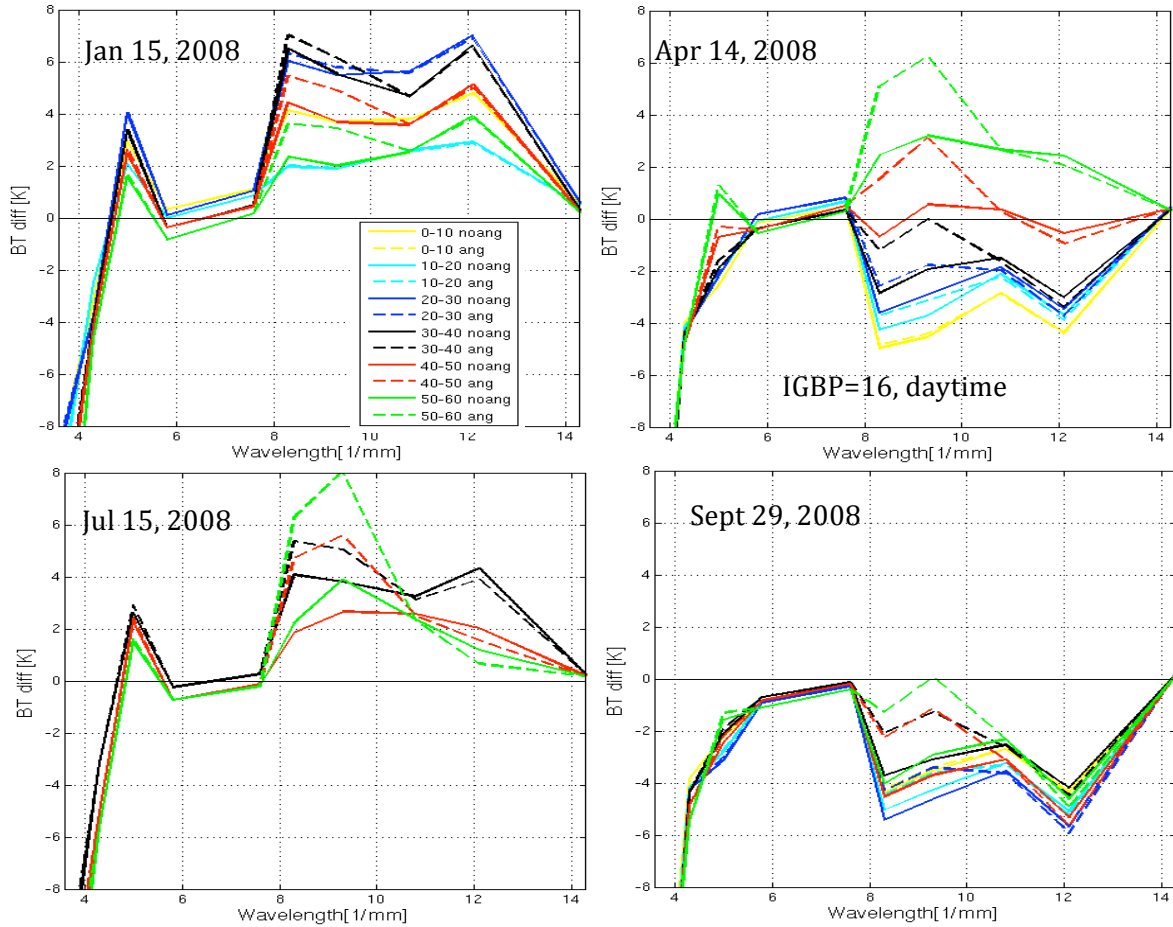

Figure 11b: same as Fugure 11a, but at day time.

However over daytime, not taking into account the short wave region where solar contamination causes large negative biases, the overestimations in the forward model calculation in January and July alternate with the spring and fall underestimation. When the underestimation occurs, the angular corrections decrease the biases significantly, as on September 29, for over 40 degrees and April 14 below the 40 degree satellite zenith angle. Generally, the magnitude of the biases are much larger (4-6K) than over the night time (0-2K).

Since the largest variation happens at the Restrahlen band, we were investigating how the different IGBP ecosystem categories behave at the 8.3 **μ**m spectral region. In Figure 12, the mean brightness temperature differences are plotted at 8.3 **μ**m for all 18 IGBP categories as a function of satellite zenith angle on Sept 29, 2008, separated by day and night. To simplify the plot, the IGBP categories are split into two categories: the top two panels illustrate the mean BT differences (biases) for the IGBP 1-8 categories and the bottom two panels for the IGBP 9-18 categories. Figure 12a shows the biases when no angular correction function has been applied while Figure 12b shows the biases when the angular correction function has been applied. Over nighttime, the biases increase for almost all ecosystem categories over the 30 degree satellite zenith angle; over daytime the trends are not so obvious. Improvements (decreasing the bias) by applying the IR emissivity viewing angle correction function can be seen only at daytime for IGBP16 (Barren/Desert Land, solid red), IGBP9 (Savanna, solid blue) and IGBP 7 (Open Shrubs, dashed black) over the 40 degree viewing angle. The bias improvement was 2.5 K for viewing angle larger than 50 degree on that day. Appendix A includes figures similar to Fig 12, but for Jan15, Apr 14, and Jul 15, 2008.
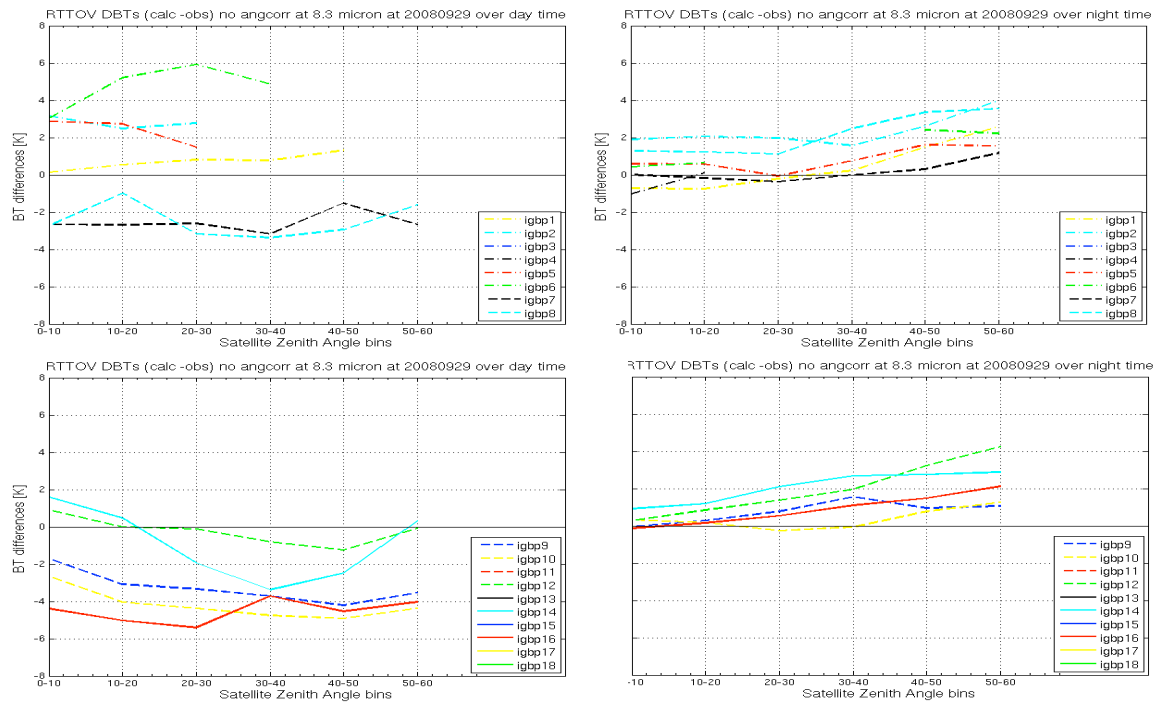
Figure 12a: Mean brightness temperature differences without any IR emissivity angular correction application at 8.3 **μ**m for all 18 IGBP categories as a function of satellite zenith angle on Sept 29, 2008, separated by day (left panels) and night (right panels). The top two panels illustrate the mean BT differences (biases) for the IGBP 1-8 categories and the bottom two panels for the IGBP 9-18 categories.
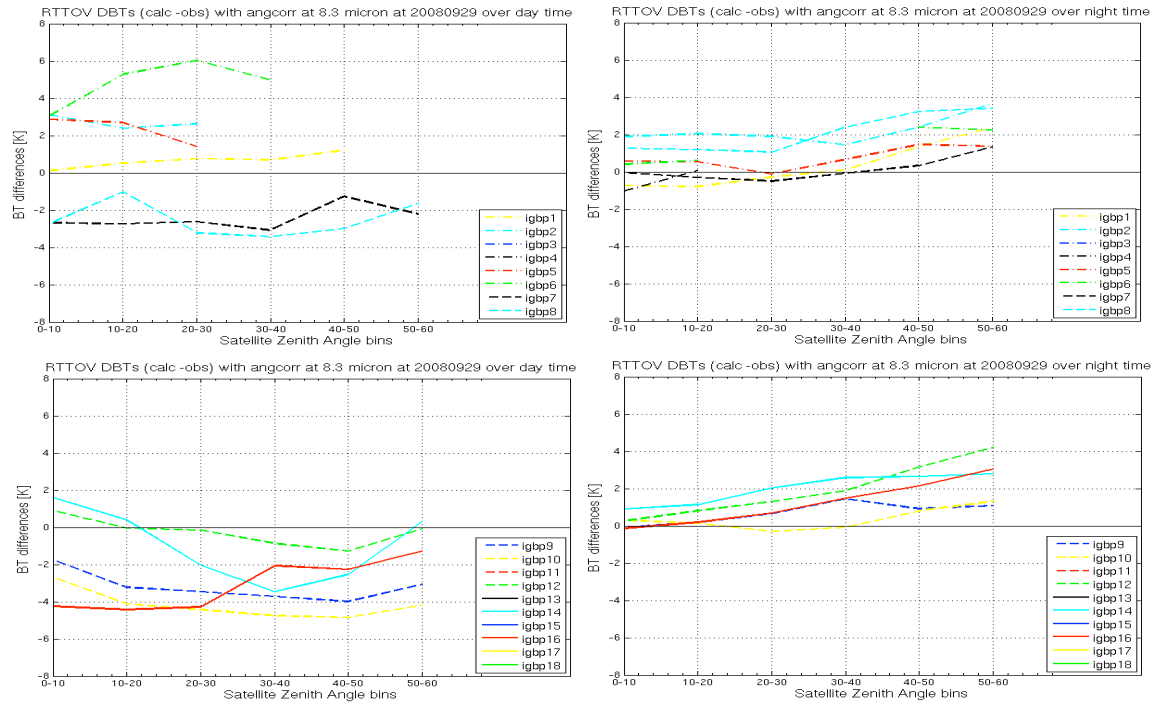
Figure 12b: same as Figure 12a, but the IR emissivity viewing angular correction was applied in the forward model calculation.

Although the angular correction function behaved as we expected from the CrIS study, its effect was not always positive for the forward model calculation. Since the RTTOV study showed positive effects only for September 29 and April 15, 2008 daytime (at the Restrahlen band) and the positive effects were significant for IGBP 7, 9 and 16 categories, the RTTOV UWIREMIS module will apply the angular correction for those IGBP categories and only for spring and fall seasons during the daytime. Negative effects were obtained for nighttime over the IGBP 16 category, when the RTTOV calculation overestimates the observations. Beyond these cases the angular correction caused neutral, or not significant effects. These results suggest that the nature of the angular correction also depends on the nature of the forward model biases which is not consistent or related to the biases of the CrIS Dual Regression retrievals we used to develop the angular correction function in this study. In the future, it would be worth investigating the effect of building an angular correction function based on RTTOV calculated brightness temperatures.

7. Conclusions and future plans

Laboratory measurement studies (Label and Stoll, 1991; Sobrino and Cuenca, 1999; Cuenca and Sobrino, 2004; Garcia-Santos et al., 2012) show an angular variation in thermal IR emissivity in the 8- 14 μm spectral band for non vegetated soils and samples, while homogeneous grass, for example, does not show angular dependence. All studies agree that the 8-9 μm restrahlen bands are the most sensitive to the angular dependence and the sand sample shows the greatest variation. They showed that in the thermal IR region, the

18

emissivity decreases with increasing viewing angle. Garcia-Santos et al. (2012) and Ruston et al (2008) also found that the zenithal emissivity change was small for viewing angles lower than 40 degrees, but after which the emissivity decreased significantly. Garcia-Santos et al. (2012) also established a relationship to take into account the zenithal dependencies for soil types.

In this NWP-SAF Associate Scientist mission, the land surface IR emissivity angular dependence has been also investigated but as compared to previous studies in the literature, it was performed on real satellite retrieved measurements and over the whole infrared spectrum. The objective of this new study was to investigate the satellite zenith angular dependence of the IR emissivity and, if there is a significant effect, to develop a parameterization correction to the monthly mean RTTOV UW IREMIS atlas for input to RTTOV (v12 and later).

The CrIS emissivity retrievals derived by the UW dual regression algorithm (Smith et al, 2011) were studied against the satellite zenith angle as a function of IGBP ecosystem types, wavelengths and seasons. Four months of CrIS data have been processed. We have found that the angular dependence differs with surface types and wavelength:

- *the most sensitive IGBP ecosystem categories are the non vegetated ones:* Barren/Desert Land (16, less than 60^0 Latitude), Savanna (9), Open Shrubs (7), and at 12.1μm the Urban Area (13). We have also found that in daytime the less vegetated surface types are mostly pronounced, while at nighttime, some forest types also show significant changes.
- *Over the Sahara desert area, the most emissivity changes occur in the spectral region between 3.7 and 9.3 μm.* They showed that emissivity increases as the satellite zenith angle increases. The magnitude and direction of the slope of the emissivity at 10.8 μm however depends on the IGBP eco system type. The longer wavelengths (12.1 and 14.3 μm) also show some changes, but with less magnitude and the emissivity mostly decreases by the satellite zenith angle.

- *Globally, at both day- and nighttime, emissivity increases occur at wavelengths less than 10.8 μm and decreases occur at the longer wavelengths* with the exception of the Urban Area (IGBP 13) for daytime spring and summer and the deciduous forests (IGBP 3 and 4) for night time winter and spring. In addition, the longer wavelengths decreasing change is more dominant at night time than in daytime.

Our results in the thermal IR spectral region over non-vegetated areas agree with the previous studies made on laboratory measurements: the thermal IR emissivity decreases when the satellite zenith angle increases. However, the magnitude of the emissivity change is different because of the different nature of the datasets: our results show larger angular changes. Additionally, the aircraft ARIES measurements (section 5) over eastern England also agree with our theory that the angular dependence differs with wavelength. Unfortunately, in the literature, we did not find any angular emissivity study over the shorter wavelength region to confirm our emissivity increase theory.

During the evaluation of the angular correction function on calculated IASI brightness temperatures over four selected days we have found that in spite of the angular correction function behaved as we expected from the CrIS study, its effect was not always positive for

the forward model calculation. Since the RTTOV study showed positive effect only for September 29 and April 15, 2008 daytime (at the Restrahen band) and the positive effects were significant for IGBP 7, 9 and 16 categories only, the angular correction function of the RTTOV UWIREMIS module is recommended to use for only those IGBP categories and only for spring and fall seasons during the daytime. Negative effects were obtained for nighttime over the IGBP 16 category, when the RTTOV calculation overestimates the observations. Beyond these cases the angular correction caused neutral, or not significant effects. These results suggest that the nature of the angular correction also depends on the nature of the forward model biases, which is not consistent or related to the biases of the CrIS Dual Regression retrievals we used to develop the angular correction function in this study. In the future, it would be worth investigating the effect of building an angular correction function based on RTTOV calculated brightness temperatures.

In the future we are planning to (1) extend our validation on CrIS BT calculations, (2) to investigate the effect of building an angular correction function based on the RTTOV calculated brightness temperatures, (3) to compare our results with other in-situ measurements, the AERIBAGO, which were taken over 12 locations in the USA, in May 2013. (4) To enhance the angular correction function, a more accurate ecosystem map should be used with possible seasonal changes. (5) The UWiremis database is based on the monthly mean MODIS Emissivity products (MOD11), which does not include enough information to perform a viewing angle dependence study. Only the new version called Collection 6 MOD11 or MOD21 product will include such a dataset. To perform a similar study with the collection 6 MOD11/MOD21 data would provide a good validation set in the future.

8. References

Belward, A.S., Estes, J.E., and Kline, K.D., 1999, The IGBP-DIS 1-Km Land-Cover Data Set DISCover: A Project Overview: *Photogrammetric Engineering and Remote Sensing* , v. 65, no. 9, p. 1013-1020.

Borbas, E.E., R. O. Knuteson, S. W. Seemann, E. Weisz, L. Moy, and H.-L. Huang, 2007: A high spectral resolution global land surface infrared emissivity database. Joint 2007 EUMETSAT Meteorological Satellite Conference and the 15th Satellite Meteorology & Oceanography Conference of the American Meteorological Society, Amsterdam, The Netherlands, 24-28 September 2007. Available at:
http://www.ssec.wisc.edu/meetings/jointsatmet2007/pdf/borbas_emissivity_database.pdf

Borbas, E. E. and B. C. Ruston, 2010. The RTTOV UWiremis IR land surface emissivity module. *Mission Report* EUMETSAT NWPSAF-MO-VS-042.
 http://research.metoffice.gov.uk/research/interproj/nwpsaf/vs_reports/nwpsaf-mo-vs-042.pdf

Cuenca, J. and J.A. Sobrino, (2004), Experimental measurements for studying angular and spectral variation of thermal infrared emissivity, Applied Optics, Vol. 43, No. 23. Pp 4598-4602.

Garcia-Satnos, V., E. Valor, V. Caselles, M.A. Burgos, C. Coll, (2012), On the angular variation of

thermal infrared emissivity of inorganic soils, Journal of Geophys. Res., Vol 117, D19116, doi: 10.1029/2012JD017931.

Label, J., and M.P. Stoll (1991), Angular variation of land surface spectral emissivity in the thermal infrared: laboratory investigations on bare soils, Int. J. Remote Sensing, 1991, Vol. 12, No. 11, 2299-1310.

Ruston, B., F. Weng and B. Yan, (2008), Use of a One-Dimensional variation retrieval to Diagnose Estimates of Infrared and Microwave Surface Emissivity Over Land for ATOVS Sounding Instruments, IEEE Transactions on Geoscience and Remote Sensing, Vol. 46, No. 2 February, 2008.

RTTOV UWIR TD, 2010: The RTTOV UWiremis IR land surface emissivity module, technical documentation by Eva Borbas, EUMETSAT, NWP-SAF, 2010.

Salisbury, J. W. and D. M. D'Aria, 1992: Emissivity of terrestrial materials in the 8-14 μm atmospheric window. Remote Sens. Environ., 42:83–106.

Salisbury, J. W. and D. M. D'Aria, 1994: Emissivity of terrestrial materials in the 3-5 μm atmospheric window. Remote Sens. Environ., 47:345–361.

Salisbury, J. W., A. Wald, and D. M. D'Aria, 1994: Thermal-infrared remote sensing and Kirchhoff's law 1. Laboratory measurements. J. Geophys. Res., 99:11897–11911.

Seemann, S.W., Borbas, E.E., Knuteson, R.O., Stephenson, G.R. and Huang, H-L. 2008: Development of a global infrared emissivity database for application to clear sky sounding retrievals from multi-spectral satellite radiances measurements. *J. Appl. Meteorol. and Clim.* **47** *108-123.*

Smith,W.L.Sr., Weisz,E., Kireev,S.V., Zhou,D.K., Li,Z., Borbas,E.E. (2011), Dual-regression retrieval algorithm for real-time processing of satellite ultraspectral radiances, Journal of Applied Meteorology and Climatology, Volume 51, Issue 8, 1455-1476.

Sobrino, J.A., and J. Cuenca (1999), Angular variation of thermal infrared emissivity for some natural surfaces from experimental measurements, Applied Optics, Vol. 38. No. 18, pp 3931-3936.
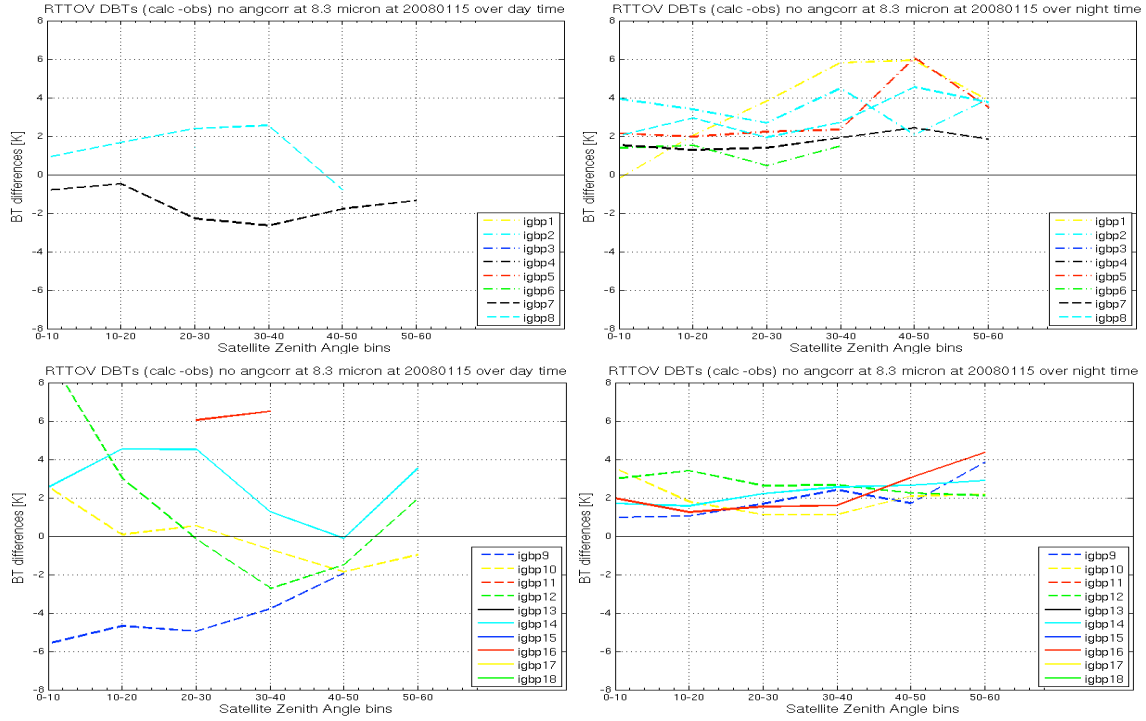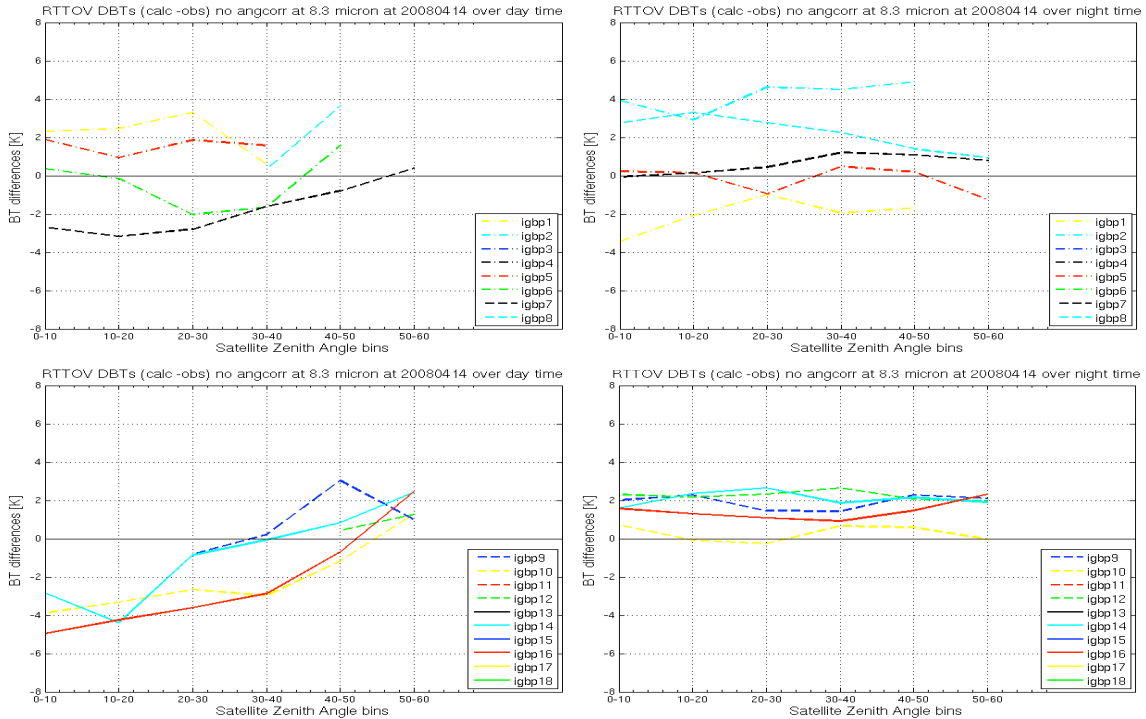
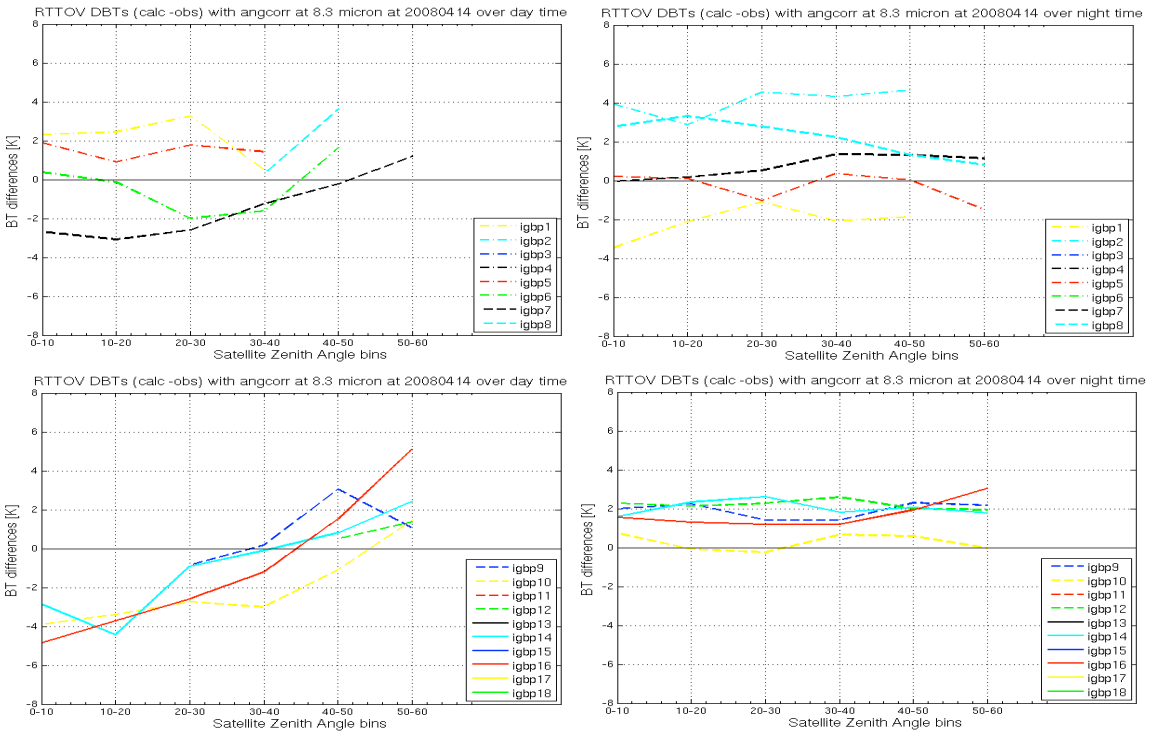**Figure 13a:** same as Figure 12a, but at January 15, 2008.
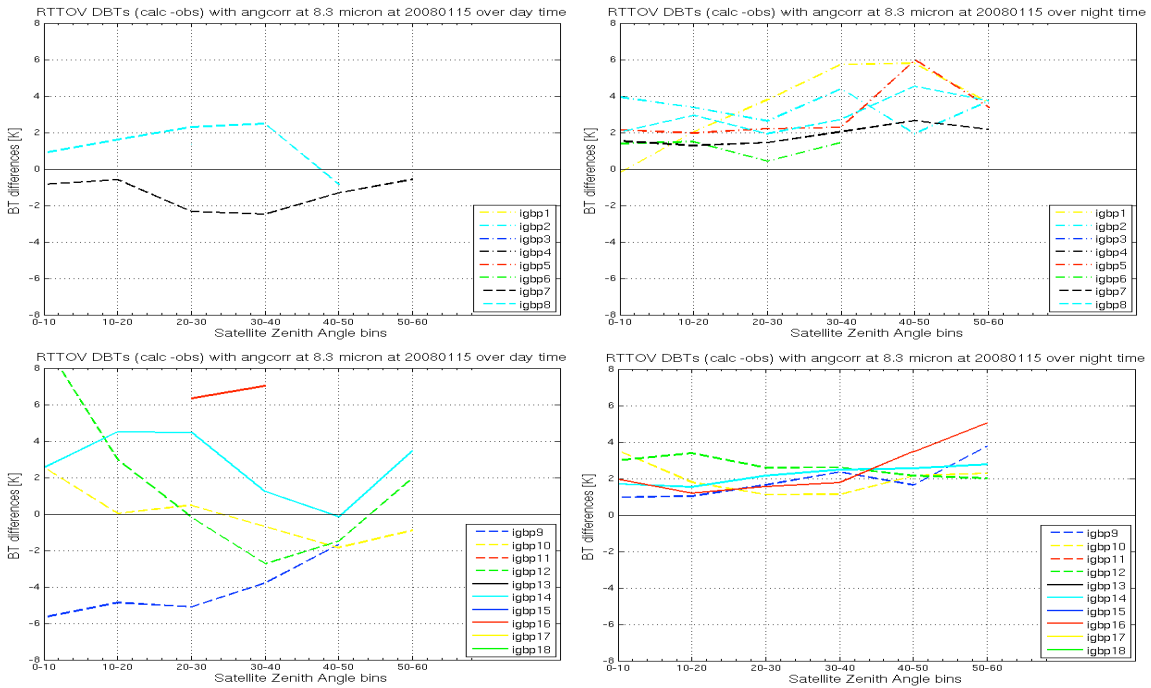
Figure 13b: same as Figure 12b, but at January 15,, 2008.

Figure 14a: same as Figure 12a, but at April 14, 2008.

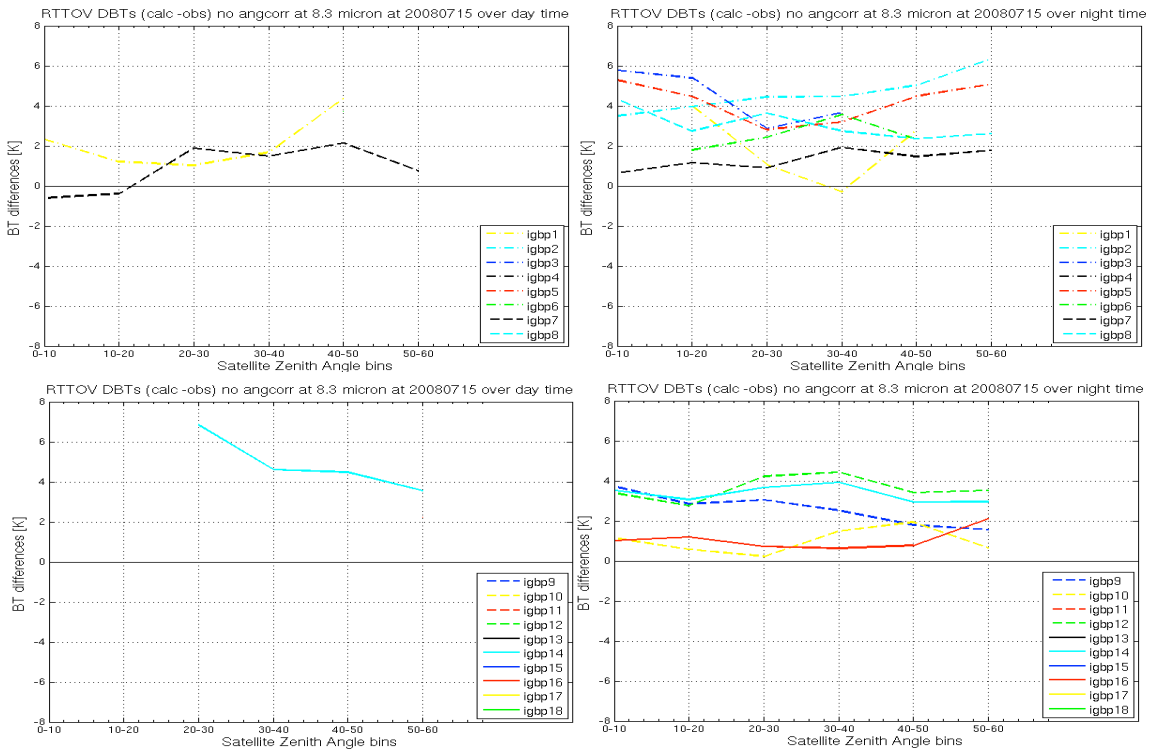**Figure 14b:** same as Figure 12b, but at April 14, 2008

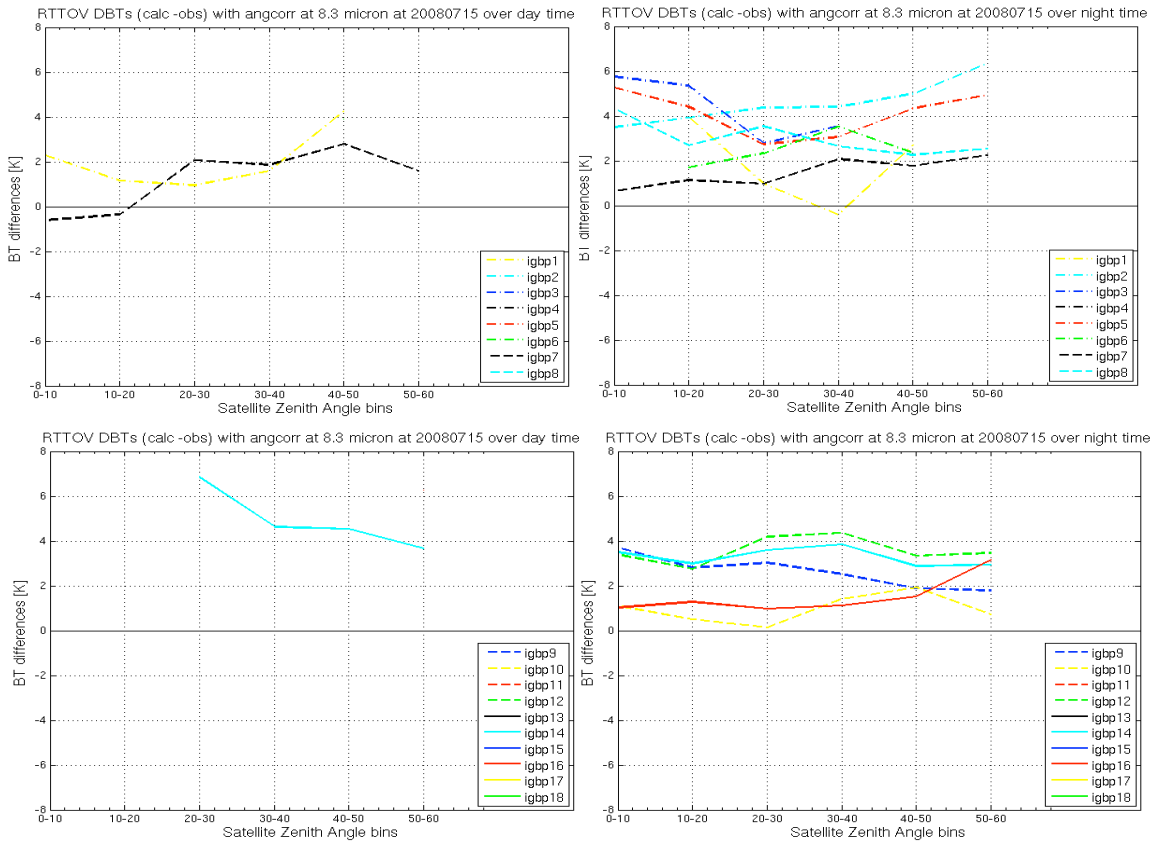**Figure 15a:** same as Figure 12a, but at July 15, 2008.

Figure 15b: same as Figure 12b, but at July 15,, 2008.